

PVP2012-78581

LBB under Beyond Design Basis Seismic Loading

Tao Zhang, Frederick W. Brust, Gery Wilkowski and Heqin Xu

Engineering Mechanics Corporation of Columbus

3518 Riverside Dr. - Suite 202

Columbus, OH 43221, USA

Alfredo A. Betervide and Oscar Mazzantini

Nucleoelectrica Argentina S. A.

Buenos Aires, Argentina

ABSTRACT

The Atucha II nuclear power plant is a unique pressurized heavy water reactor (PHWR) being constructed in Argentina. The original plant design was by Kraftwerk Union (KWU) in the 1970's using the German methodology of break preclusion. The plant construction was halted for several decades, but a recent need for power was the driver for restarting the construction. The US NRC developed leak-before-break (LBB) procedures in draft Standard Review Plan (SRP) 3.6.3 for the purpose of eliminating the need to design for dynamic effects that allowed the elimination of pipe whip restraints and jet impingement shields. This SRP was originally written in 1987 with a modest revision in 2005. The United States Nuclear Regulatory Commission (US NRC) is currently developing a draft Regulatory Guide on what is called the Transition Break Size (TBS). However, modeling crack pipe response in large complex primary piping systems under seismic loading is a difficult analysis challenge due to many factors. The initial published work on the seismic evaluations for the Atucha II plant showed that even with a seismic event with the amplitudes corresponding to the amplitudes for an event with a probability of 1e-6 per year, that a Double-Ended Guillotine Break (DEGB) was pragmatically impossible due to the incredibly high leakage rates and total loss of make-up water inventory. The critical circumferential through-wall flaw size in that case was 94-percent of the circumference.

This paper discusses further efforts to show how much higher the applied accelerations would have to be to cause a DEGB for an initial circumferential through-wall crack that was 33 percent around the circumference. This flaw length would also be easily detected by leakage and loss of make-up water inventory. These analyses showed that the applied seismic peak-ground accelerations had to exceed 25 g's for the case of this through-wall-crack to become a DEGB during a single seismic loading event. This is a factor of 80 times higher than the 1e-6 seismic

event accelerations, or 240 times higher than the safe shutdown earthquake (SSE) accelerations.

KEY WORDS: LBB, Atucha II nuclear power plant, multiple cracks, crack-pipe-element, dynamic response, seismic loading

INTRODUCTION

The Atucha II nuclear power plant is a pressurized heavy water reactor being constructed in Argentina. Nuclear power plants must be designed to maintain their integrity and performance of safety functions for a bounding set of normal operational events as well as abnormal events that might occur during the lifetime of the plant. Seismic safety against strong earthquakes is a very important issue in nuclear power plants. The piping systems are designed to have safety margins against such earthquakes. The general design criteria of the US Code of Federal regulations (10CFR50 Appendix A originally written in 1971) requires that the emergency core cooling system (ECCS) be sufficient to tolerate a double-ended guillotine break (DEGB). The US NRC developed leak-before-break (LBB) procedures in draft Standard Review Plan (SRP) 3.6.3 for the purpose of eliminating the need to design for dynamic effects that allowed the elimination of pipe whip restraints and jet impingement shields. This SRP was originally written in 1987 with a modest revision in 2005. The US NRC is currently developing a draft Regulatory Guide on what is called the Transition Break Size (TBS). The transition break size is an equivalent opening area that could be used to size the ECCS system, loss of offsite power requirements, etc rather than using the DEGB assumption. A relatively simple analysis is required using a 10^{-6} seismic loading.

Sometimes it is possible to evaluate crack growth by using the finite element method (FEM) on the basis of fracture mechanics.

However, it is difficult to analyze such a piping system under seismic loading using the conventional numerical analysis procedure based on fracture mechanics because this approach requires iterative re-meshing of the analysis model during crack growth. It is also difficult to evaluate the seismic response of cracked pipes, because the degradation behavior is complicated compared with non-degrading behavior. Thus, predicting local crack growth and the resulting seismic responses of cracked pipes in a straightforward manner is quite difficult, requiring large amount of meshes and excessive computer resources. Moreover, seismic analysis including multiple cracks even becomes more challenge. Therefore, an efficient evaluation method needs to be developed to predict crack behaviors and seismic responses. A simplified modeling technique using multiple springs, sliders, break-away elements and pin elements was developed by Olson et al. [1,2]. This original approach seemed to work reasonably well but was rather cumbersome and time consuming to implement. In recent years, a new type of element within ABAQUS [3], a connector element, was used to simulate the elastic, plastic, and post maximum load behavior of a cracked pipe (damage initiation and damage evolution) [4,5]. At the crack location, a single connector element was used compared with the complicated arrangement of springs, sliders, dashpots, etc. Analysis approach and results were validated against a series of experiments [6,7] and good agreement was obtained through the comparison between the numerical results and measured experimental data. It is confirmed that this latest development of the simplified modeling approach is applicable to a seismic analysis for a cracked pipe on the basis of fracture mechanics.

These analyses of Atucha II nuclear power plant are performed by placing developed novel cracked pipe elements into a complete model of the primary cooling system including the reactor pressure vessel, pumps, and steam generators as summarized in the paper. Fracture mechanics evaluations for the Atucha II plant under beyond design basis seismic loading showed that even with a seismic event with the amplitudes corresponding to an event with a probability of 10^{-6} per year and higher, that a DEGB was practically not possible. Some work was published early [8]. This paper summarizes detailed results and further shows how much higher the applied accelerations would have to be to cause a DEGB for an initial circumferential through-wall crack that was 33 percent (about 120°) around the circumference. This suggests there is a huge margin for beyond design basis seismic events against an instantaneous DEGB failure and the Atucha II plant rupture is pragmatically impossible.

KEY ELEMENTS IN DETERMINING IF A DEGB CAN OCCUR WITH BEYOND DESIGN BASIS SEISMIC LOADING

In this study, a full analysis of the entire Nuclear Steam Supply System (NSSS) system was conducted to determine the actual margins on DEGB under beyond design basis seismic loading. This was done to eliminate unknown degrees of conservatism of assuming load-controlled failure, properly accounting for the pipe boundary conditions (natural restraint of the pressure-induced bending), and determine how fast the DEGB might be

in an actual NSSS system. The key steps involved the following [8].

- Materials data was developed from an actual weld used in a qualification tests.
- Worst-case crack shapes were determined using the worst-case degradation mechanism. Since stress corrosion cracking (SCC) has become an issue with many PWR plants, we used an upper bounding SCC curve to both primary water stress corrosion cracking (PWSCC) and intergranular stress corrosion cracking (IGSCC). The pipe material is 20MnMoNi55 (similar to A533B) and at this time is not known to be susceptible to SCC; nevertheless, we used that very high crack growth rate so that 80 years from now if some SCC mechanism occurs we will have that degradation mechanism. SCC also gives much longer surface cracks than fatigue, so it is a more conservative mechanism for assessing LBB. This analysis required weld residual stresses to be calculated. The weld residual stress analysis procedure used was that validated by NRC-funded residual stress round-robin efforts [9]. This weld was stress-relieved (accounted for in the residual stress analyses), but had a stainless steel cladding that at operating temperature gave a higher than expected residual stress due to the differential thermal expansion [9].
- Leak-rates were calculated as a function of time with worst-case SCC crack growth rate. The crack morphology of a SCC was used for the leakage analyses. The leak detection of this heavy water plant is incredibly good compared to normal pressurized water reactor (PWR) and boiling water reactor (BWR) plants.
- The finite element (FE) model of the whole plant was constructed including the containment building and NSSS system with precise boundary conditions modeled.
- The seismic hazard curve and time-history input functions were developed for this site using US NRC and International Atomic Energy Agency (IAEA) procedures. Time-history inputs for SSE (10^{-4}) and 10^{-6} seismic event were created.
- We determined the normal operating stresses, SSE stresses and 10^{-6} seismic stresses in the entire primary pipe loop. Low damping was conservatively used and best-estimated soil foundation was used, although there were less than 2% differences in the loading of the cracked pipe even with the upper-bound soil stiffness.
- Implementation of worst-case crack shapes was done in the primary pipe loop under normal operating and different seismic loading to determine a crack size that will result in DEGB failure.
- Finally an assessment of the margins on the DEGB was made. The amount of time from the penetration of the surface crack to the DEGB was an initial goal. This was a design criterion of the boron injection system to come on line to prevent any fuel melting for the positive reactivity of this core design.

FE MODEL OF THE ATUCHA II PLANT

The details of the Atucha II PHWR were available through detailed drawings of the plant, dimensions of each segment of pipe used in the main loop, and an Inventor CAD model shown in Figure 1 (a). The NSSS model was first created in ABAQUS with all the appropriate boundary conditions modeled. Dead-weight loads compared well to the original KWU design calculations done by hand. Figure 1 (b) shows the ABAQUS NSSS model and some of the support and boundary conditions imposed. There are 1,992 elements and 2,669 nodes in the *Emc²* ABAQUS NSSS model that includes pipe, beam and elbow elements for the primary pipe loop. By using the cracked-pipe element methodology [5], a single connector element can be added for a crack location. Typically cracks were put in 4 locations, so that was a trivial increase in the FE mesh size.

The containment building model was created by James J. Johnson and Associates in ANSYS from drawings supplied by Nucleoelectrica Argentina Sociedad Anonima (NA-SA). The ABAQUS NSSS model was converted to an ANSYS [10] FE model. The stand-alone ANSYS NSSS model was benchmarked against the ABAQUS model. Support locations and boundary conditions were verified to be as modeled. A comparison of the natural frequencies and mode shapes of the NSSS models was made. This was a great check of all the geometry and boundary conditions, and resulted in very good comparison of the mode shapes and natural frequencies. After the benchmarking process, the ANSYS NSSS model was inserted into the reactor building FE model, see Figure 1(c).

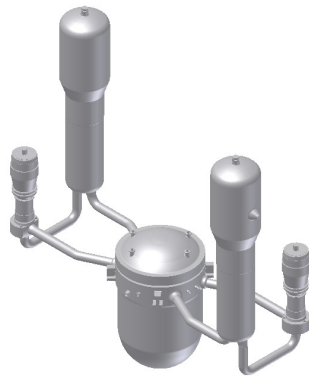
The process of a crack growth in the piping system can experience starting with surface-crack growth through the thickness and subsequently transitioning to a circumferential through-wall crack, and finally from a through-wall crack to a complete pipe break. Figure 2(a) schematically shows the moment-rotation curve for a pipe with a circumferential surface-crack developing to a circumferential through-wall crack. The crack experiences elastic loading, plastic deformation, reaches the maximum load capacity, and then grows the crack through the thickness. Figure 2(b) is the moment-rotation curve for a pipe with a circumferential through-wall crack from loading until break. It is seen that the load capacity decreases after reaching the maximum point. The whole process from a surface crack to through-wall crack and break is schematically presented in Figure 2(c). From surface crack transition to a through-wall crack, there is often a sudden decrease in load depending on the surface crack length. It is the moment versus rotation due to the crack that is calculated by various fracture mechanics analyses and then implemented into the “cracked-pipe element (CPE)”. During the early 1990’s, multiple springs, slider and pin elements in ANSYS had to be used to simulate the whole process in the International Piping Integrity Research Group (IPIRG) program as shown in Figure 3 [1]. In recent years, a new type element of ABAQUS, connector element, was used to simulate the elastic, plastic, and post maximum load (damage) behavior of a crack until breakage occurs as shown in Figure 4. In addition, this type of element can define admissible relative motion, which can be used to simulate the over-closure of a crack, i.e., when the crack faces come in contact under compressive loading, the pipe takes the

compressive loads as if it was un-cracked. It should be noted that the use of this element is a major improvement compared to the procedure used in past NRC/IPIRG programs using ANSYS where a series of springs and dashpots were required. This highly efficient “cracked-pipe element” methodology can be used to represent the global moment versus rotation due to crack response. The analysis was validated against many different separate-effect pipe tests (i.e., pure bending, bending and pressure, cyclic loading, dynamic loading, etc.) as well as some more complex pipe-system experiments [4, 5]. Numerical comparisons between finite element analysis (FEA) predictions and experimental measurements show, in general, a *well-defined* connector element can capture the static and dynamic behavior under monotonic and cyclic loading. The methodology allows for a single element to be used in the FE analysis at each crack location and account for crack growth during the analysis.

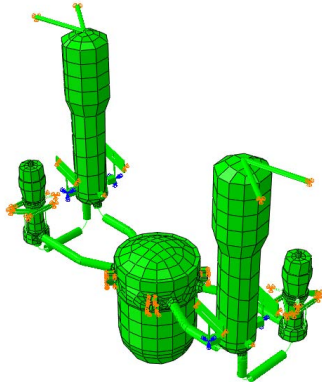
The procedure for determining the CPE response is then:

1. Determine the Ramberg-Osgood material parameters for the base metal.
2. Determine the J-resistance curve for the weld material at seismic loading conditions.
3. Choose a crack size to analyze. The crack sizes considered were systematically increased in size since we could not produce a pipe break.
4. Use the NRCPIPE/NRCPIPES [8] fracture analysis code with the above material parameters, using the correct pipe and crack geometries, and determine the moment versus pipe-rotation-due-to-crack to be inserted at each crack.
5. The moment rotation curves are input of a CPE using the ABAQUS connector element. The analyses performed here used 4 cracks in the primary piping and all cracks were placed at nozzle welds.
6. The dynamic analysis was performed using ABAQUS Implicit solution procedure. The initial conditions for each seismic modeling consist of the initial operating stresses (gravity, internal pressure, and thermal expansion loads).
7. The analyses are performed throughout the 10 second seismic event because for this study the strong motion duration was between 3–6 seconds and the behavior of the cracked pipes was examined to determine if failure occurred.

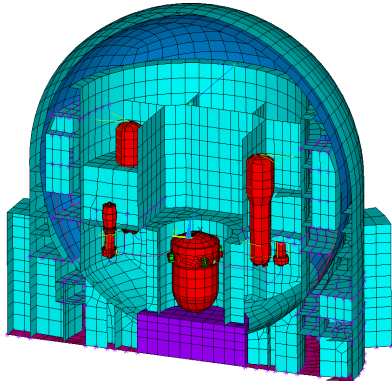
The CPE moment versus rotation-due-to-crack is then inserted into the Atucha II pipe system at crack locations (multiple cracks can be inserted) shown in Figure 5. The coordinate systems shown in Figure 5 represent the four locations where cracks were introduced. Note that these are on different loops so that they do not interact.



(a) NSSS system



(b) FE model of NSSS system



(c) with containment building

Figure 1 FE model of NSSS system and containment building

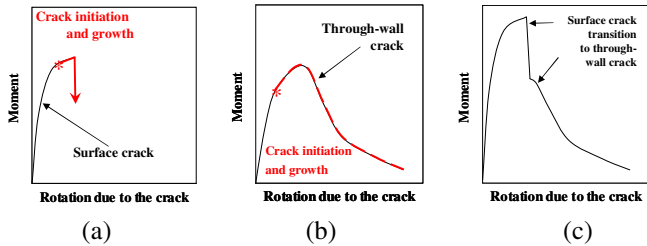


Figure 2 Moment versus rotation-due-to-the-crack curves from initial loading to full break of a pipe with a circumferential crack

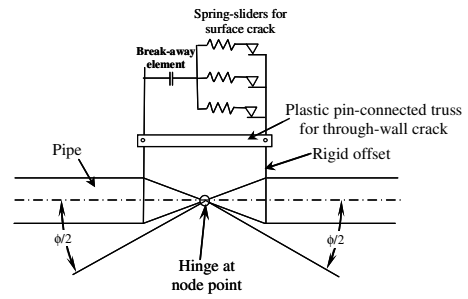


Figure 3 Simulation of a crack in IPIRG program during the early 1990's

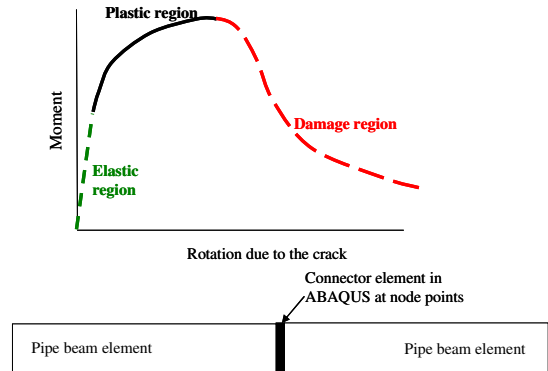


Figure 4 Simulation of a crack in current program using ABAQUS with validation in separate-effect pipe tests

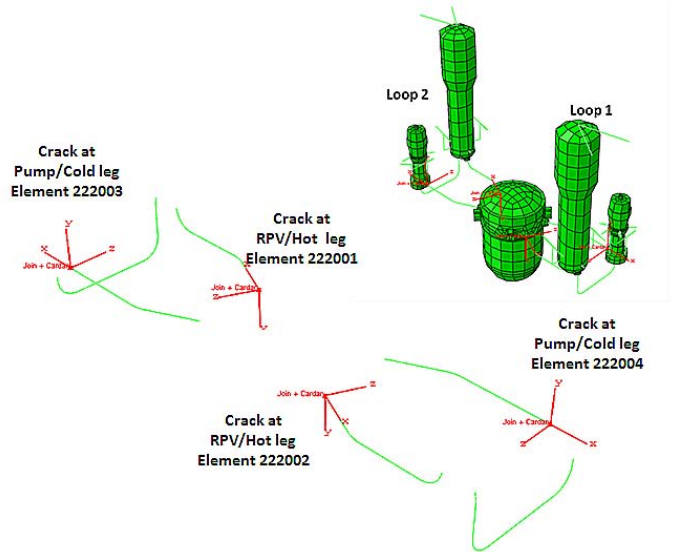


Figure 5 Crack pipe element locations in primary piping with element numbers

RESULTS OF BEYOND DESIGN BASIS SEISMIC ANALYSIS

A series of analyses of the nuclear steam supply system (NSSS) for SSE and the 10^{-6} seismic event loading were conducted. Extensive sensitivity studies with various crack angles have been performed. The different circumferential through-wall

crack sizes studied were 55.5°, 152.8°, 180°, 210°, 225° and 229.5°. Additional crack sizes were also considered. For brevity, some of results of 10^6 seismic event loading are summarized below.

The analyses consist of inserting four cracks at weld locations in the hot legs of the RPV and cold legs of the pump in the model for each seismic run. These cracks keep increasing in size as the original purpose was to find a crack size that would lead to a complete primary system pipe break. Figure 6, Figure 7, Figure 8, Figure 9, and Figure 10 show the moment and rotation relations for 55.5-degree, 152.8-degree, 180-degree, 210-degree and 229.5-degree circumferential through-wall cracks, respectively.

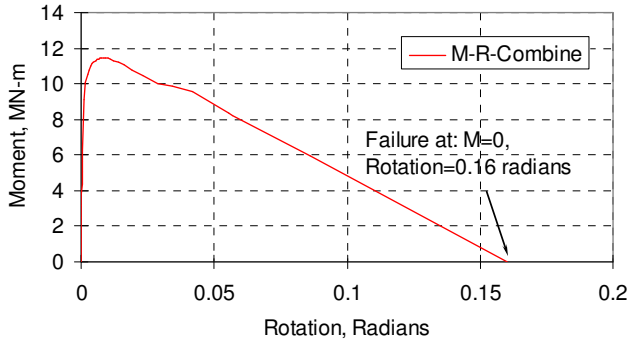


Figure 6 Moment versus rotation due to the crack for 55.5-degree circumferential through-wall crack

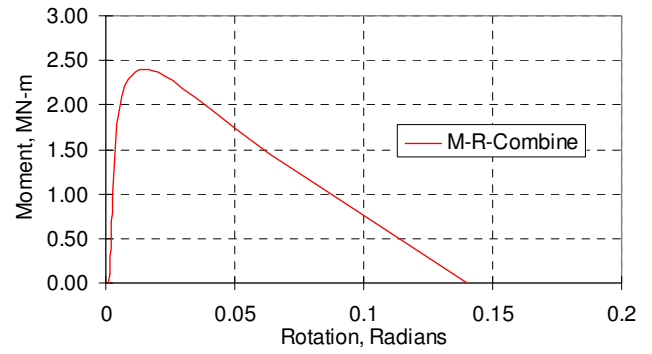


Figure 8 Moment versus rotation due to the crack for 180-degree circumferential through-wall crack

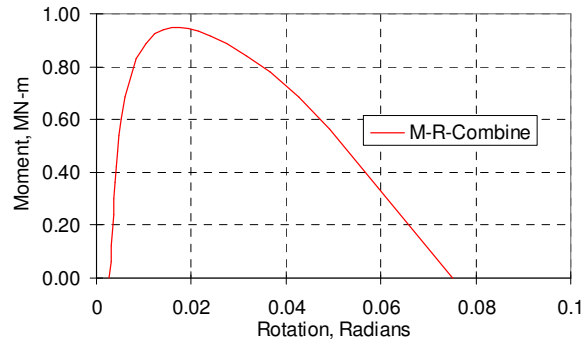


Figure 9 Moment versus rotation due to the crack for 210-degree circumferential through-wall crack

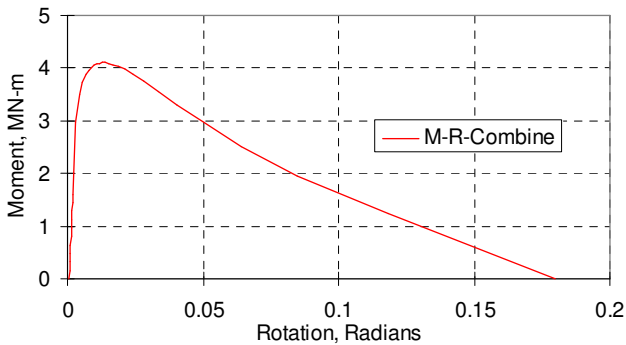


Figure 7 Moment versus rotation due to the crack for 152.8-degree circumferential through-wall crack

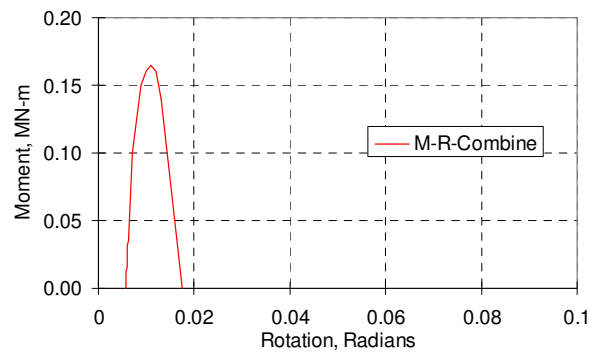


Figure 10 Moment versus rotation due to the crack for 229.5-degree circumferential through-wall crack

These cracked-pipe element (CPE) properties are obtained by implementing the J-resistance curve and performing J-estimation analyses using the LBB.ENG2 method [8] for a circumferential through-wall cracked pipe in bending with axial tension from the pressure loading. The internal pressure of the

pipe has been considered when the CPE moment-rotation relationship was developed. Figure 6 through Figure 10 show the initial offset of the pressure loads on the moment versus rotation behavior. This initial offset becomes more visible for the 180-degree and bigger crack lengths used. The larger cracks have lower moment and rotation capacity, as expected. The maximum-moment capacity is about 11.43 MN-m for the 55-degree crack while the maximum moment capacity for the 229.5-degree crack is about 0.165 MN-m. Originally, this offset was included in the moment rotation response of the CPE. However, as modeling continued and we realized that crack breaking was very difficult because of the constraint of the piping system, it was realized that this initial offset cannot occur in the constrained piping system. As such, this offset was removed in the CPE definition. However, the effect on results was negligible.

Figure 11 provides the dynamic moment-rotation responses for the 55.5-degree circumferential through-wall crack under the given seismic excitation. The maximum moments, which are along the blue curve, are located at Element 222003 (the pump weld of the cold leg in Loop 2). (Note, the crack element numbering definitions are given in Figure 5). The crack experiences an elastic response when this 55.5-degree crack is used in the analysis. The maximum moment is about 4.0 MN-m while the maximum moment for crack initiation (from the LBB.ENG2 analysis) is 11.4 MN-m. Notice that Figure 11 represents the input moment rotation response (red curve) of the CPE (from Figure 6) and it is seen that the crack response at all four CPE locations simply cycles between about a maximum of 4 MN-m to -1 MN-m. In other words, the response is elastic and stays on the low portion of the curve where no crack damage can take place. If failure were predicted for this crack size, the predicted moment-versus-rotation curve shown in Figure 6 would go to zero moment at a crack pipe rotation of 0.16 radians. This analysis also predicted no crack growth and a pipe break will not occur.

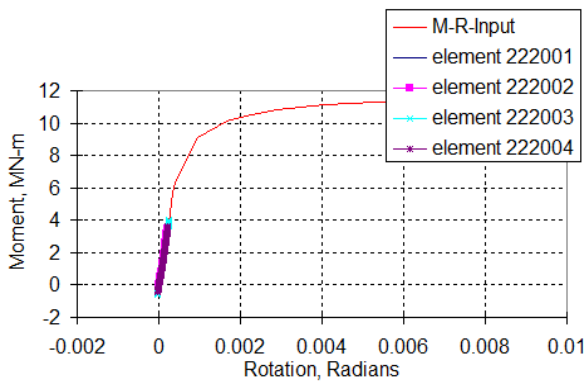


Figure 11 Moment versus rotation histories at different locations for 55.5 - degree circumferential through-wall crack with embedment effects and best-estimated soil properties using free-field motion artificial time histories

Since this crack did not even get close to breaking the pipe, the next crack size considered was much larger (152.8-degree). Recall that the initial crack considered (55.5 – degree) is a very conservative estimate of the initial through-wall-crack (TWC)

that would develop under the worst stress corrosion cracking scenario. Figure 12 shows the dynamic moment-rotation responses for the 152.8-degree circumferential through-wall crack. For the best soil estimate 10^{-6} UHS seismic excitation, the crack also experiences an elastic response as seen in Figure 12. The maximum moment developed from the 10^{-6} seismic loading is also located at Element 222003, i.e., the pump weld of cold leg in Loop 2. The maximum developed moment is about 2.35 MN-m while the maximum moment capacity for the 152.8-degree circumferential through-wall crack is about 4.1 MN-m. The maximum moment predicted to develop with the 55-degree crack was 4.0 MN-m while the maximum moment to develop seismically for this 152.8-degree crack is 2.35 MN-m. This is because the entire primary system and vessels cause the cracks to respond more to a ‘displacement’ type loading than load-controlled loading. The crack response to load control (i.e., the cracked pipe fails immediately at maximum load) compared to that for a displacement-control loading is markedly worse. Under displacement control there is actually ‘load shedding’ due to the stiffness change at the cracked section, which reduces the severity of the crack tip conditions. This result is quite good for the Atucha II design.

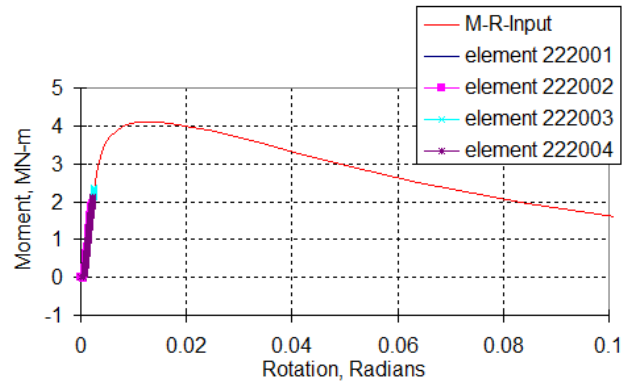


Figure 12 Moment versus rotation histories at different locations for 152.8 - degree circumferential through-wall crack with embedment effects and best-estimated soil properties using free-field motion artificial time histories

Figure 13 shows the results for the 180-degree circumferential through-wall-crack case. Maximum moment response also happens at Element 222003 which is the pump weld location of the cold leg of Loop 2. The maximum moment value is about 1.91 MN-m. The maximum moment developed seismically becomes smaller compared to the 152.8-degree and 55.5-degree crack cases due to the nature of displacement control with the lower stiffness at the cracked pipe section. However, the cracked pipe sections undergo some small plastic deformation with this crack length. Note the initial offset in the input moment rotation curve at zero moment. This is due to the initial pressure loading applied with the load control LBB.ENG2 J-estimation method. As discussed above, this offset would not be realized in the Atucha II piping system due to constraint. When the model was re-run with this pressure induced offset removed the results were not affected.

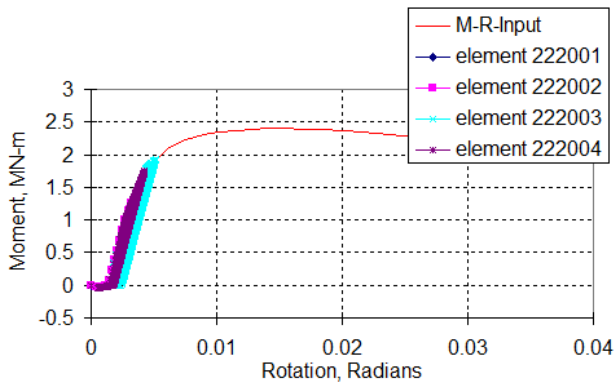


Figure 13 Moment versus rotation histories at different locations for 180 - degree circumferential through-wall crack with embedment effects and best- estimated soil properties using free-field motion artificial time histories

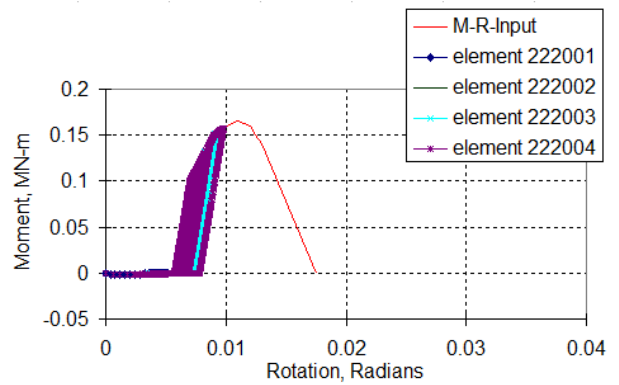


Figure 15 Moment versus rotation histories at different locations for 229.5 - degree circumferential through-wall crack with embedment effects and best- estimated soil properties using free-field motion artificial time histories

Figure 14 gives the results of dynamic responses for the 210-degree circumferential through-wall crack case. For this case, the maximum developed moment takes place at Element 222004, which is the pump weld of the cold leg of Loop 1. The maximum moment developed seismically is about 0.75 MN-m while the maximum moment-capacity of the cracked pipe is about 0.95 MN-m. When compared to the 180-degree case, more plastic deformation was developed during this longer crack analysis. Figure 15 is the dynamic responses for the 229.5-degree circumferential through-wall crack cases. As expected, this case shows more plastic deformation is developed under the same 10^{-6} seismic event. However, the maximum moment capacity of the cracked pipe sections was never reached, therefore, no crack initiation occurs.

As discussed above, extensive sensitivity studies with various crack angles were carried out. The different circumferential through-wall crack sizes evaluated with the cracked-pipe element approach were 55.5°, 152.8°, 180°, 210°, 225° and 229.5°. The 229.5-degree crack is the largest crack whose moment-rotation relation can be obtained through conventional J-estimation analyses using the LBB.ENG2 method, which includes pressure (axial tension loading) and unconstrained bending. Note the zero-offset comes from the unconstrained end-rotations from the pressure loading. For larger crack sizes (greater than 229.5 degrees) with unconstrained bending (i.e., free rotation at the pipe ends) the cracked pipe breaks due to pressure alone from the LBB.ENG2 analysis.

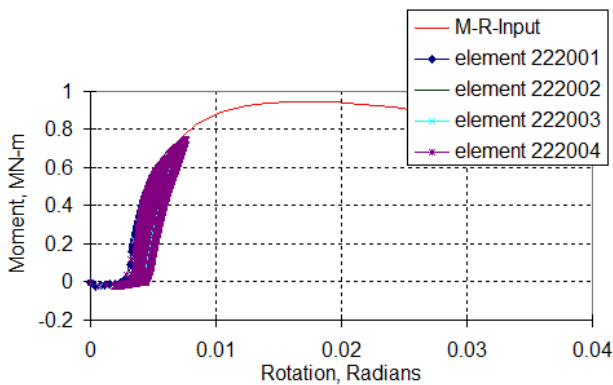


Figure 14 Moment versus rotation histories at different locations for 210 - degree circumferential through-wall crack with embedment effects and best- estimated soil properties using free-field motion artificial time histories

As an additional sensitivity study, a case of 320-degree crack was modeled where pressure was neglected (i.e., pure bending only). Figure 16 is the input moment and rotation relations for 320-degree cracks obtained from LBB.ENG2 method with no internal pressure. Without including pressure, it is seen that the moment-rotation curves start from the origin. The maximum moment capacity for the 320-degree crack is about 0.06 MN-m if no pressure effect is considered. These may be slightly higher than the true behavior of incorporating pressure with the constrained rotation effects. Figure 17 shows the results for the 320-degree circumferential through-wall-crack case. The maximum developed moment also takes place at Element 222004. The maximum moment developed seismically is about 0.059 MN-m while the maximum moment-capacity of the cracked pipe is about 0.06 MN-m. There are some numerical errors for Element 222003 and Element 222004 which do not follow the input moment-rotation exactly (they go a little higher) as seen in Figure 17. For this run, the overall moment and rotation responses follow the input moment-rotation curve. The maximum moment capacity of the cracked-pipe sections was never reached for these cases. However, there was slight crack growth in these analyses since the crack initiation load occurs at about 90% of maximum load.

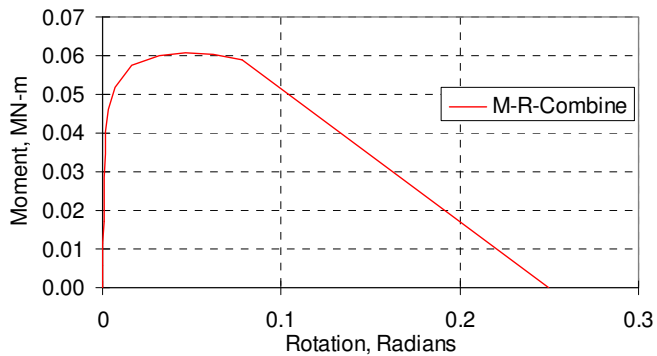


Figure 16 Moment versus rotation due to crack relation for 320-degree crack without pressure effect from LBB.ENG2 pure-bending analysis

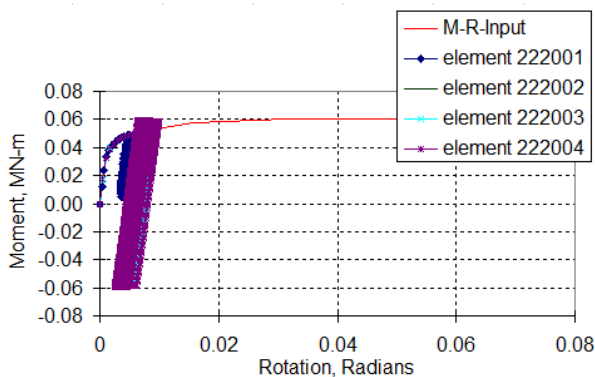


Figure 17 Moment versus rotation histories at different locations for 320-degree crack with embedment effects and best-estimated soil properties using as free-field motion artificial time histories (without pressure offset) – using cracked-pipe element analysis from LBB-ENG2 for pure bending

One could see that the peak seismic moments being applied 10^{-6} seismic events were continually decreasing as the crack size increased. Typical LBB analyses assume the uncracked pipe stresses are maintained in the presence of the crack and are load-controlled for stability analyses. These crack lengths were becoming so large, that they were beyond the range where the LBB.ENG2 J-estimation scheme was validated by experimental data, and certainly not using experimental data under combined bending and pressure with restrained ends. The key result and observation from these analyses are that the entire primary system and vessels cause the cracks to respond more like a ‘displacement’ type loading than load-controlled loading. The crack response under load control (i.e., the cracked pipe fails immediately at maximum load) compared to that for a displacement-control loading is markedly worse. Under displacement control there is actually ‘load shedding’ due to the stiffness change at the cracked section, which reduces the severity of the crack tip conditions. This result is incredibly good for the Atucha II design – as well as other nuclear power plants. Additionally, the results from the IPIRG pipe-system tests showed that with restrained rotation, pressure causes the

critical crack size to be ~95% of the circumference (342-degrees), so having the 270 and 320-degree cracks being stable is consistent with those results [1, 2].

Another main interest is to find out the safety margin for beyond design basis seismic events against an instantaneous DEGB failure. Also the triggering of the fast boron injection system needs the *cyclic crack opening area* to be determined precisely so that the boron injection system will trigger *before* rapid DEGB of the pipe system. An initial 120-degree circumferential through-wall crack was selected for the sensitivity analysis. This flaw length, 33 percent around circumference, would be easily detected by leakage and loss of make-up water inventory.

When extreme beyond design analysis seismic loading was applied, the crack will have to experience extremely large crack opening and closing and numerical difficulties were encountered. Extensive efforts were spent investigating the numerical behavior of crack over-closure, reverse plasticity and damage evolution. A crack can not become over-closure, and the reverse plasticity is assumed not to introduce damage initiation and damage evolution while the tensile loading is the main driving force for crack growth. Therefore, a second connector element has to be introduced to overcome the numerical instabilities.

A series of large seismic excitations were applied to the NSSS model. The seismic response, particularly the post-damage behavior, of excitations of 6.72g (21 times the $10e-6$ case), 9.6g (30 times the $10e-6$ case), 12.8g (40 times the $10e-6$ case) and 25.6g (80 times the $10e-6$ case) for the 120-degree crack were investigated. For the brevity, only the results of 25.6g (80 times the $10e-6$ case) are reported here. Figure 18 shows significant damage evolution was developed according to the moment and rotation responses at crack locations. Figure 19 shows the rotation history at Element 222003 (the pump weld of cold leg in Loop 2) and Element 222004 (the pump weld of the cold leg in Loop 1) which experienced a larger damage. Between them, the crack at Element 222003 (the pump weld of the cold leg in Loop 2) experienced the largest damage; the crack opening was up to 0.368 radians while the crack can tolerate 0.43 radians as the largest crack opening. Since the reverse plasticity was a numerical issue, comparison was also made if connector element can (1) only have elastic plus damage evolution and (2) elastic plus reverse plasticity and damage evolution. The results were shown in Figure 20 and Figure 21. The legend with adjusted plasticity indicates the results for the case of elastic plus reverse plasticity and damage evolution, the legend with ‘E’ indicates the results for the case of only having elastic and damage evolution while the curve with legend including ‘P’ shows the results for the case of elastic, plasticity in tension and damage evolution. The last case is more of physical meaning. It is interesting that all these cases lead to virtually the same crack rotation (crack opening) history. This is also mainly due to the fact that the whole structure responds to the seismic excitation as like-displacement-control. Certainly it should be noted that the moment values for different cases are different even though the rotation histories appear to be very similar. However, to trigger the boron injection system, the rotation history (i.e., the

crack opening) plays a critical role as the leakage rate and its calculation are based on crack opening history.

For Atucha II power plant, the boron injection system becomes active under 25.6g (80 times of the 10e-6 seismic excitation, or 240 times higher than the SSE accelerations). Obviously such type of seismic excitation does not physically exist or, at the least, the probability of such an earthquake is extremely low. This also suggests there is a huge margin for beyond design basis seismic events and the Atucha II plant rupture is pragmatically impossible.

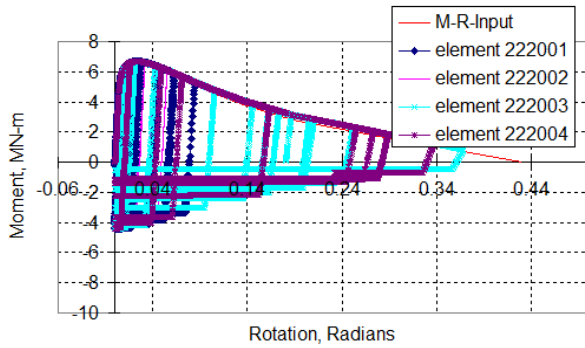


Figure 18 Moment versus rotation histories at different locations for 120-degree crack under 80 times higher than the 1e-6 seismic event accelerations

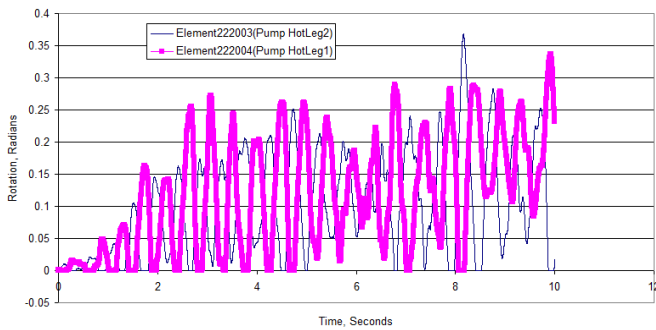


Figure 19 Moment versus rotation histories at different locations for 120-degree crack under 80 times higher than the 1e-6 seismic event accelerations

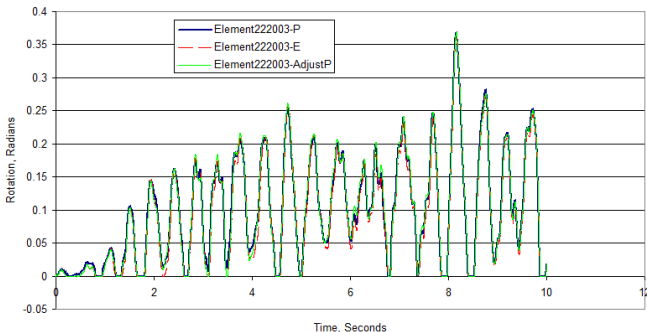


Figure 20 Rotation history comparisons for different cases at pump weld of loop 2 for 120-degree crack under 80 times higher than the 1e-6 seismic event accelerations

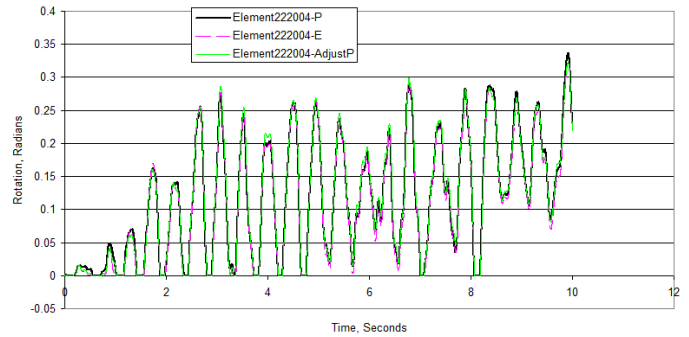


Figure 21 Rotation history comparisons for different cases at pump weld of loop 1 for 120-degree crack under 80 times higher than the 1e-6 seismic event accelerations

SUMMARY AND CONCLUSION

Seismic fracture mechanics evaluations were conducted for the Atucha II plant and results showed that even with a seismic event with the amplitudes corresponding to an event with a probability of 1e-6 per year and higher, that a DEGB was pragmatically impossible. These analyses are performed by placing cracked pipe elements into a complete model of the primary cooling system including the reactor pressure vessel, pumps, and steam generators as summarized in the paper.

This paper further shows the very high safety margin when the applied accelerations would have to be to cause a DEGB for an initial circumferential through-wall crack that was 33 percent (about 120°) around the circumference. These analyses showed that the applied seismic peak-ground accelerations had to exceed 25.6 g's for the case of this through-wall crack to become a DEGB during a single seismic loading event. This is a factor of 80 times higher than the 1e-6 seismic event accelerations, or 240 times higher than the SSE accelerations. This suggests there is a huge margin for beyond design basis seismic events and pragmatically an instantaneous DEGB in the primary pipe loop cannot happen in this plant. These surprising results and efficient methodology have important implications for other nuclear power plants as well.

ACKNOWLEDGEMENTS

The authors would like to thank NA-SA in Argentina for their support of the work.

REFERENCES

- 1 Olson, R., Scott, P. and Wilkowski, G., "Application of a Nonlinear-Spring Element to Analysis of Circumferentially Cracked Pipe Under Dynamic Loading," *ASME Pressure Vessels and Piping Conference*, June 21-25, 1992, New Orleans, LA, USA.
- 2 Olson, R., Wolterman, R., Scott, P., Krishnaswamy, P. and Wilkowski, G., 1994, "The Next Generation Analysis Methodology for Cracked Pipe Systems Subjected to

- Dynamic Loads,” *ASME Pressure Vessels and Piping Conference*, June 19-23, 1994, Minneapolis, MN, USA.
- 3 ABAQUS 6.10-1, Dassault Systemes Simulia Corp, 2010.
 - 4 Zhang, T., Brust, F. W., Shim, D. J., Wilkowski, G, Nie, J., and Hofmayer, C., NRC NUREG/CR-7015 (BNL-NUREG-91346-2010) report: “Analysis of JNES Seismic Tests on Degraded Piping”, July, 2010.
 - 5 Zhang, T., Brust, F. W., Wilkowski, G, Shim, D. J., Nie, J., Hofmayer, C. and Ali, S., “Numerical Analysis of JNES Seismic Tests on Degraded Combined Piping System”, *ASME Journal of Pressure Vessel Technology*, Vol. 134, February 2012, pp. 011801-01~12.
 - 6 Suzuki, K., Kawauchi, H., and Abe, H., “Test Programs For Degraded Core Shroud and BWR Piping (Simulated Crack Models And Input Seismic Waves For Shaking Test),” *ASME Pressure Vessels and Piping Conference*, July 23-27, 2006, Vancouver, BC, Canada.
 - 7 Suzuki, K. and Kawauchi, H., “Test Programs for Degraded Core Shroud and PLR System Piping (Seismic Test Results and Discussion on JSME Rules Application),” *2008 ASME PVP conference*, July 27-31, Chicago, IL, USA.
 - 8 Wilkowski, G., Brust, F., Zhang, T., Hattery, G., Kalyanam, S., Shim, D., Kurth, E., Hioe, H., Uddin, M., Johnson, J., Maslenikov, O., Gurpinar, A., Asfura, A., Sumodobila, B., Betervide, A. and Mazzantini, O., “Robust LBB Analysis for Atucha II Nuclear Plant,” *2011 ASME PVP conference*, July 17-21, 2011, Baltimore, MD, USA.
 - 9 Zhang, T., Brust, F. and Wilkowski, G., “Weld Residual Stress in Large Diameter Nuclear Nozzles”, *2011 ASME Pressure Vessels and Piping Division Conference*, July 17-21, 2011, Baltimore, MD, USA.
 - 10 Ansys 11.0, ANSYS, Inc.